SPACE TELESCOPE SCIENCE INSTITUTE
Operated for NASA by AURA

Instrument Science Report ACS 2004-006

Time Dependence of ACS WFC CTE Corrections for Photometry and Future Predictions

Adam Riess, Jennifer Mack
May 5, 2004

ABSTRACT

We present measurements of photometric losses due to imperfect parallel and serial CTE on ACS WFC on 3 distinct dates: March 2003, August 2003, and February 2004. Improvements in our method of measuring the photometric losses are discussed. At all dates we see strong evidence for photometric losses in the parallel direction whose values grow with decreasing stellar flux and background. We see evidence for a modest increase in these photometric losses with time. We provide a global fitting formula to correct for CTE losses for all flux levels, sky values, and times. We continue to see no evidence of loss along the serial direction (as expected). The photometric losses from imperfect parallel CTE decrease with increasing aperture size (likely) due to the ability of large apertures to recapture a fraction of the trapped and emitted charge. We extrapolate our time-dependent correction formula to the end of the decade and predict that for the vast majority of science applications the use of CTE correction formulae will retain the precision of flux measurements to better than a few percent.

1. Introduction

The unrelenting flux of damaging radiation in the HST environment produces an ever increasing population of charge traps in the silicon-based CCD's and decreases their charge transfer efficiency (CTE). This ongoing degradation was seen for WFPC2 (Whitmore et al., 1999) and STIS (Goudfrooij & Kimble, 2002) and can be expected for both

Copyright© 1999 The Association of Universities for Research in Astronomy, Inc. All Rights Reserved.

optical channels of ACS: WFC and HRC. Previously we reported on the photometric corrections for point sources due to imperfect CTE on ACS as derived from on-orbit data taken in March 2003, one year after installation (Riess, ISR ACS 2003-009). This analysis provided a single calibration applicable to images obtained in close temporal proximity to the CTE measurement. For temporal extrapolations of the CTE calibration, internal CTE data (cosmic rays tails and the extended-pixel response data) predicted a linear growth rate. However, to determine more accurate CTE calibrations applicable to past and future cycles, it is necessary to continue to track the unpredictable loss of CTE and derive its time-dependence. With the time-dependence well established, interpolation of CTE corrections at the time of any GO observation will be more precise, and the future condition of CTE on ACS can be projected.

2. Observations

As in March 2003, we undertook a calibration program (now GO 10043, previously GO 9648; P.I. Riess) to obtain a sequence of observations of the off-core field (6’ West) of the rich cluster 47 Tuc (00h 22m 37.2s +/- 1", -72d 4’ 14" +/- 1”). As before, our goal for each camera was to compare the relative photometry of individual stars as a function of the number of pixel transfers during read-out. We direct the reader to Riess (ISR ACS 2003-009) for details of the observing sequence. For reference and to serve as a reminder, we reprint Figure 1 which illustrates the sequence of observations and direction of read-out which provides the dependence of photometry on pixel transfers.

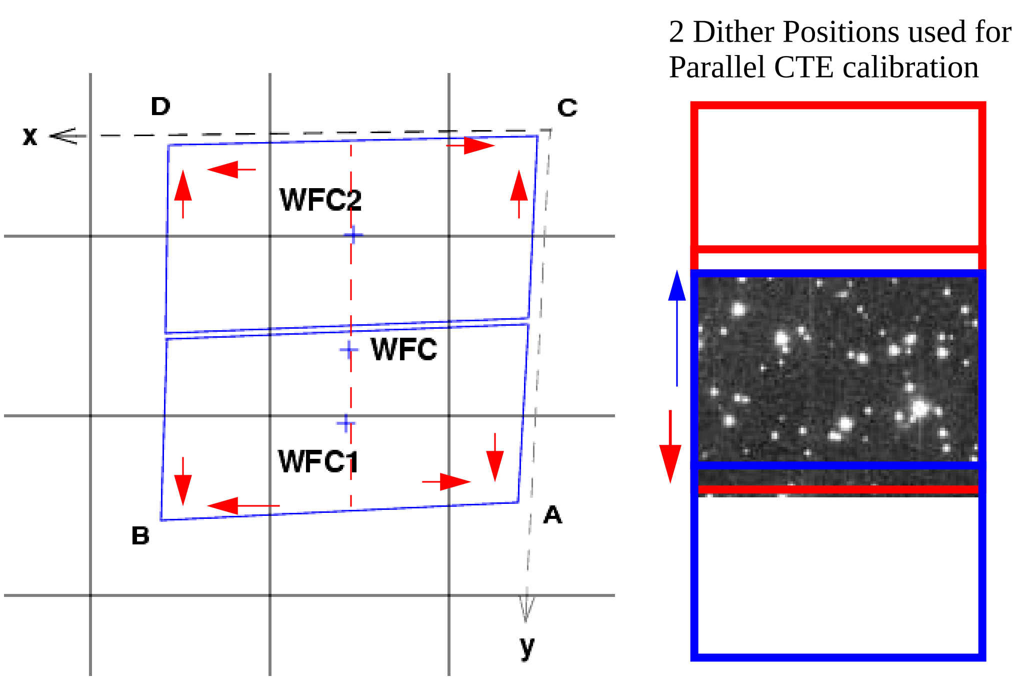

Figure 1: Schematic showing the location of the read-out amplifiers and the WFC direction of read-out. The right panel illustrates the two pointings used to vary the number of parallel transfers for individual stars.

3. Analysis

During the current analysis a number of improvements in the methods used by Riess (2003) were found and implemented including a reanalysis of the data from the first iteration of the CTE calibration from March 2003. We describe the improvements here.

Purity of Star Lists

Previously, star lists were auto-generated from an IDL implementation of DAOfind (find.pro). Stars were selected as positive fluctuations surpassing a threshold of 0.05e/sec and satisfying sharpness and roundness thresholds. A problem with these lists was the spurious inclusion of multiple "sources" in the region of very bright stars resulting from artifacts such as airy disk peaks, diffraction spikes, and saturated regions. The contamination was ~10% of the sample. To fix this problem, we masked 50 pixel radius regions around bright stars and discarded stars found within these regions.

Locality of Sky

Previously, a single sky value for the whole frame was determined from a sigma-clipped mean. Errors due to a sky gradient intrinsic to 47 Tuc would be removed in difference photometry of a fixed point source. However, scattered light could introduce a non-repeating sky gradient (whose scale and location depends on orbital parameters). To account for the effects of scattered light we now use local, individual sky measurements taken to be the median counts in annuli of inner radius 10 pixels and outer radius 15 pixels centered on each star. The noise in individual sky measurements is larger than the previous, global sky, but it should now be free from the aforementioned potential scattered light problem and any uncertainty in the bias subtraction performed by the ACS calibration pipeline.

Recentering

CTE smears the observed charge distribution along the read-out direction, changing estimates of the center or centroid of a star. Previously, we attempted to retain the true, unperturbed center positions of the stars by using their positions in the master star list (allowing only for a single, global registration error of each frame). Further consideration has led us to now recenter on each individual star before doing photometry. *Recentering is desirable to mimic the process undertaken by GO's who can be expected to estimate the center of a source from a CTE-effected image before measuring its flux.*

4. WFC Results

We can expect the WFC on ACS to be more strongly impacted by imperfect CTE than the HRC due to its greater number of pixel transfers (2048 vs. 1024). WFC is also utilized an order of magnitude more frequently than HRC. As a result, we have chosen to prioritize the analysis of the WFC time dependent CTE. Subsequent studies will focus on the other less urgent but addressable subjects of the external CTE monitoring program: the time dependence of CTE for HRC and the impact of postflashing on photometric losses due to imperfect CTE.

Aside from the aforementioned changes in the analysis procedure (i.e., recentering, local sky, and purity of star lists) our procedure was identical to the one described in Riess (2003) and for the sake of brevity is not repeated in detail here. For each combination of filter (F606W, F775W, and F502N) and exposure time (30 and 400 seconds), difference magnitudes of stars in flux bins (2 magnitudes wide) were regressed against their pixel transfer differences to determine the flux loss rate resulting from read-out. To account for spurious flux differences due to cosmic-ray impacts, outliers were discarded and a robust, least-absolute-deviation (LAD) statistic was used to perform the linear regression. (The LAD results were checked against a least-squares, sigma clipped fit.) The analysis was performed independently for apertures with 3, 5, and 7 pixel radii.

The resulting linear relationships and their sky and stellar flux levels were used to determine the best parameters A, B, and C in the parallel (Y-direction) CTE parameterizations used in Riess (2003):

$$YCTE = 10^{A} \times SKY^{B} \times FLUX^{C} \times \frac{Y}{2048} \qquad (1)$$

The term, Y/2048 reflects the linear relationship with pixel transfer of the CTE loss.

Table 1 contains the best fit values of the parameters A, B, and C and their uncertainties for equation (1) for 3 different aperture sizes and for 3 dates; March 2003, August 2003, and Feb 2004. Figure 2 shows the relationships between YCTE and stellar flux at different sky levels for the 3 dates. The new fitted relationships for the first calibration, March 2003, are consistent with those reported for this date in Riess (2003), with one noteworthy difference: for faint stars (< 1000 electrons) in the presence of substantial background (> a few tens of electrons/pixel), losses due to imperfect CTE are mitigated (i.e., the B-parameter is significantly negative). This behavior is expected as it has been seen on WFPC2 and STIS. The weakness and even absence of such a trend reported by Riess (2003) was surprising. The change in the results can be traced to the adoption of a local sky measurement and its ability to remove either scattered light or the quadrant bias offset, either of which may have affected the initial results. As further confirmation of this result, we see the same significant dependence on background in the two more recent datasets.

Table 1: CTE Correction Coefficients for WFC Parallel Transfer

A(σ)	B(σ)	C(σ)	ap
March 2003			
-0.27(0.22)	-0.29(0.04)	-0.44(0.07)	3
1.32(0.33)	-0.34(0.04)	-1.05(0.13)	5
1.02(0.40)	-0.33(0.05)	-0.85(0.14)	7
August 2003			
A(σ)	**B(σ)**	**C(σ)**	**ap**
-0.38(0.39)	-0.27(0.09)	-0.45(0.12)	3
-0.30(0.18)	-0.27(0.04)	-0.41(0.05)	5
-0.64(0.23)	-0.31(0.06)	-0.28(0.07)	7
February 2004			
A(σ)	**B(σ)**	**C(σ)**	**ap**
-0.89(0.56)	-0.26(0.14)	-0.30(0.18)	3
-1.42(0.35)	-0.43(0.07)	-0.09(0.10)	5
-1.05(0.43)	-0.30(0.09)	-0.19(0.13)	7

After comparison of the PSF with model PSF's from Tiny Tim (Krist, private communication), we concluded that the telescope was moderately out of focus in the Aug 2003 epoch causing the unrealistic negative magnitude losses seen for bright stars at high background (where none would be expected) as seen in Figure 2. The field dependence of the PSF encircled energy weakens as the aperture size increases, but at a radius of 3 pixels the focus position (and the accompanying coma and astigmatism) may have caused a ~1% underestimate of the losses at this date.

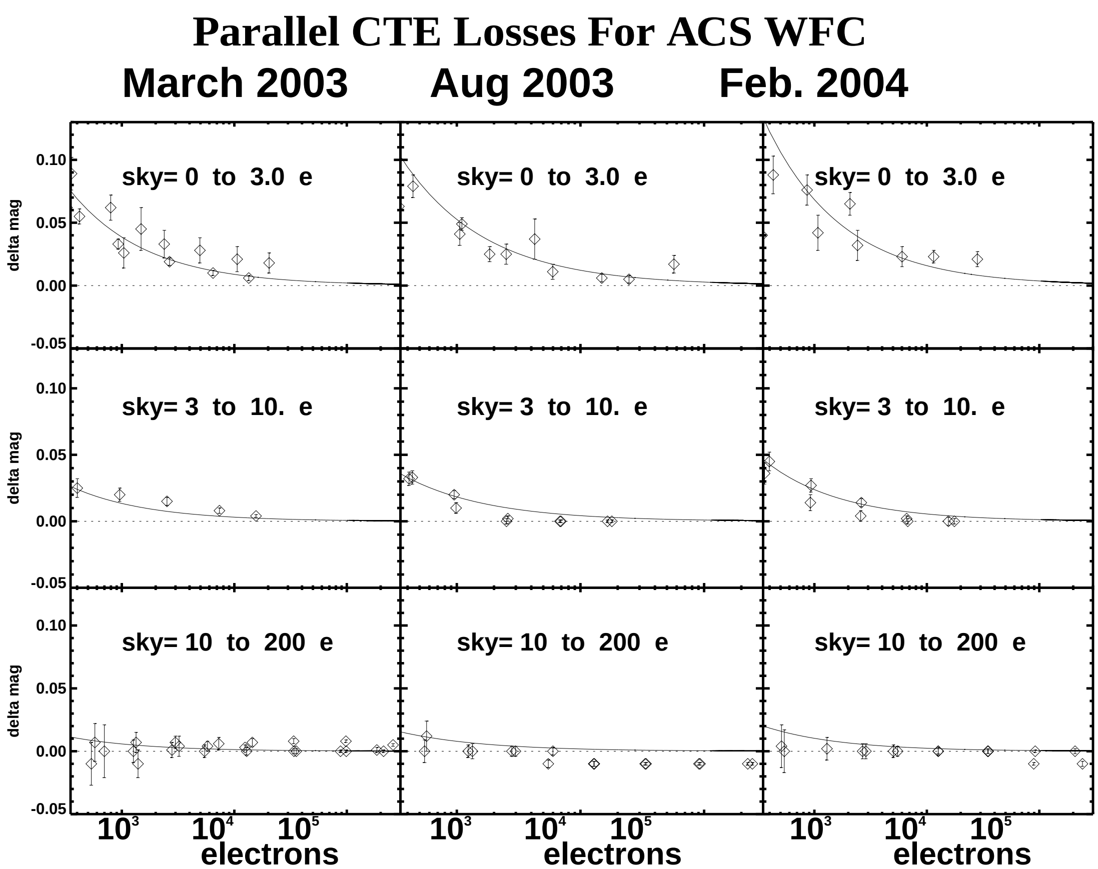

Figure 2: Parallel CTE trends. The rows and columns show the photometric losses (at y=2048) for different sky levels and dates, respectively for aperture radii of 3 pixels. The fitted line uses the global, time-dependent correction formula (2) with the appropriate stellar flux and sky levels.

Figure 3 shows the best parameterizations of the dependence of photometric loss on stellar flux for the 3 different dates. These models use the best fit parameters shown in Table 1 for equation (1). For higher flux levels (>1000 e) any differences for the 3 different dates are not statistically significant. For low flux levels (<300 e) the fits likely reflect true degradation with time.

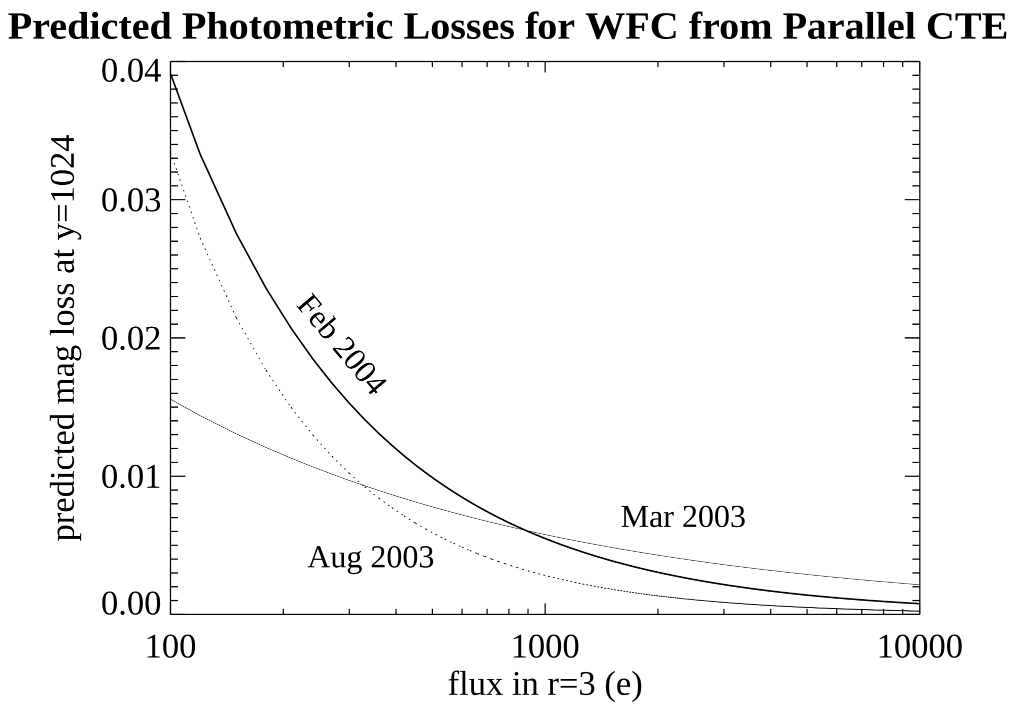

Figure 3: The predicted photometric losses for WFC due to imperfect parallel CTE at y=1024. Best fit parameters of the form of equation (1) for 3 dates were determined and the predicted dependence on stellar flux is shown. Note that the predictions here are for halfway across the chip (y=1024) which are half the size of those across the full chip (y=2048) as shown in Figures 2 and 4. The adopted sky value is 20 e.

For serial CTE (i.e., losses which depend on the number of X pixel transfers) the photometric data from all three dates at all stellar flux levels and background values remain consistent with no significant net flux loss, as seen in Figure 4. This is the same result found by Riess (2003) and is not surprising given the results from WFPC2 and STIS for which losses due to imperfect serial CTE were an order of magnitude smaller than for imperfect parallel CTE. This result is also corroborated by the internal CTE data comparing serial and parallel CTE (i.e., cosmic-ray tails; Riess 2003 and extended pixel response; Mutchler, private communication 2004). We will continue to monitor the serial CTE for changes. For now we recommend no corrections be made for imperfect serial CTE.

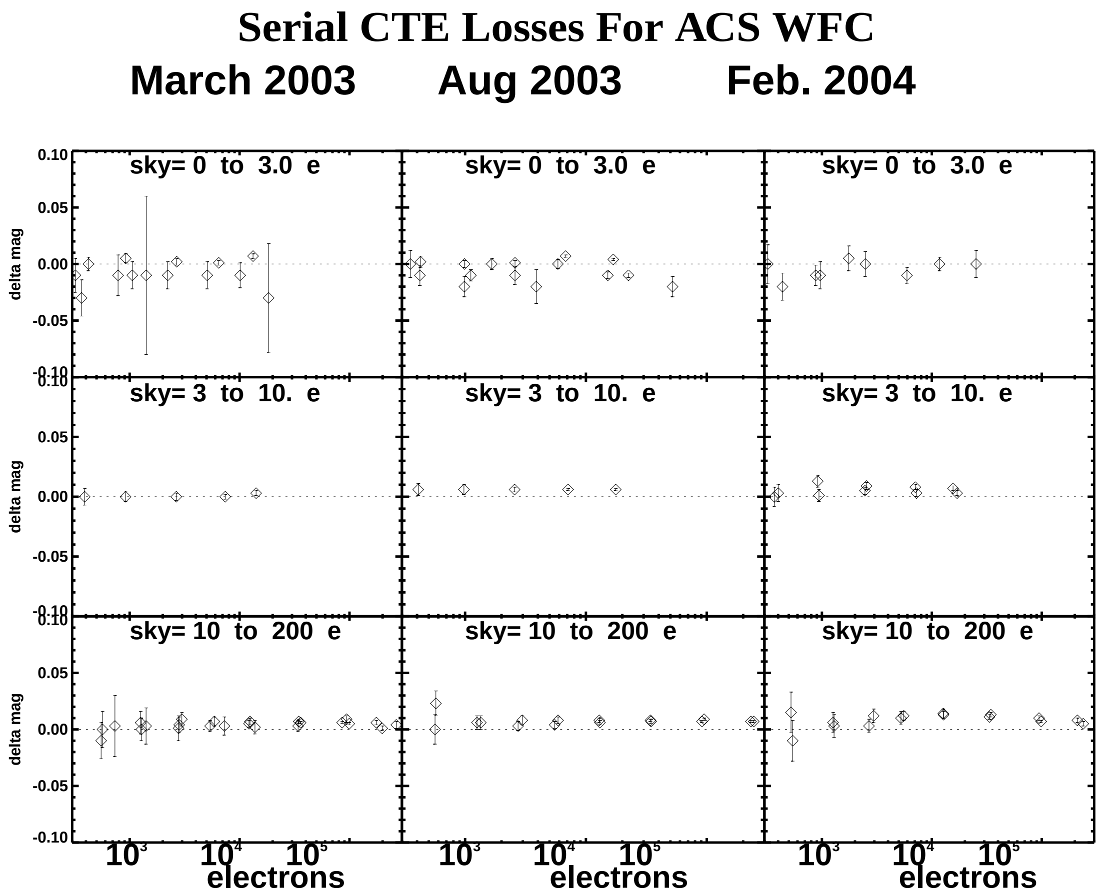

Figure 4: Serial CTE trends. The rows and columns show the photometric losses at x=2048) for different background levels and dates, respectively for r=3 pixels. To date we see no evidence of photometric losses caused by imperfect serial CTE.

5. Time Dependence of Parallel CTE on WFC

The estimates of photometric losses due to imperfect CTE at individual epochs are relatively noisy, and with only three independent measurements over a time baseline of 1 year, it is difficult to reliably extract a functional form for the time dependence. Nevertheless, the data do indicate an increase in the loss over the course of the year of monitoring, as seen in the top two rows (lowest background) and the lowest stellar fluxes of Figure 2.

If we naively assume the losses at the time the camera was installed were nil, and we assume a *linear* increase in photometric losses (based on the internal CTE metrics as well as experience from WFPC2 and STIS), we can derive a single global fit to the 3 epochs using a simple time dependence. Using formula (2), we rederived these global coefficients and provide them in Table 2. Fits using the global correction formula are shown in Figure 2.

$$YCTE = 10^A \times SKY^B \times FLUX^C \times \frac{Y}{2048} \times \frac{(MJD - 52333)}{365} \quad (2)$$

Table 2: Global, time-dependent CTE Correction Coefficients for WFC

A(σ)	B(σ)	C(σ)	ap
0.14(0.14)	-0.31(0.02)	-0.64(0.05)	3
-0.55(0.15)	-0.32(0.03)	-0.40(0.04)	5
-0.70(0.24)	-0.34(0.04)	-036(0.07)	7

Figure 5 shows the dependence of loss on background for the global correction formula (with an aperture radius of 3 pixels). Background appears to have the greatest mitigating power for faint stars.

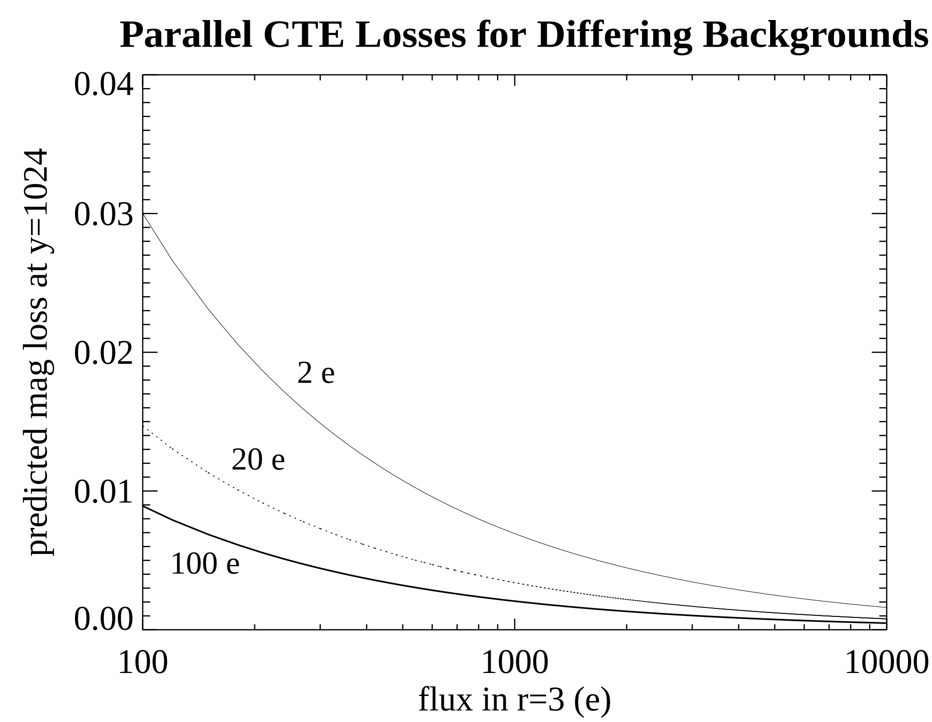

Figure 5: As Figure 3, but now showing the predicted photometric loss from parallel CTE, *1 year after launch*, for different sky levels.

Figure 6 shows the dependence of loss on aperture size from the global correction formula. Interestingly, the loss decreases as the aperture size increases. The likely explanation for this effect is that a significant fraction of the charge which is trapped is emitted on the read-out timescale. A greater fraction of lost charge is then collected in larger apertures.

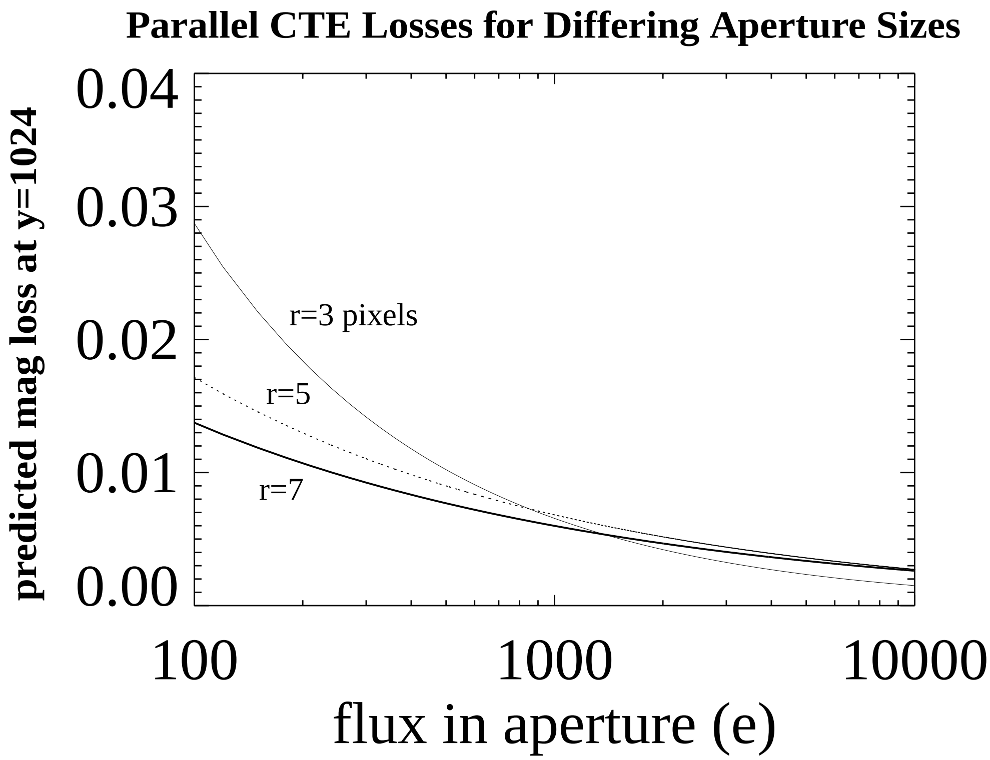

Figure 6: Predicted losses at y=1024, *2 years after launch*, for different aperture sizes. Losses decrease as aperture size increases, likely because larger apertures collect trapped charge that is reemitted in close proximity to the charge packet. The adopted sky value is 20 e.

6. Recommendation

At the present time, we encourage users to estimate their CTE losses from the global, time-dependent correction formula. To utilize this formula, users need to calculate the background level and stellar flux of their source in electrons (not electrons per second) for the appropriate aperture size for each exposure. They also need to determine the position of their source relative to the read-out amplifiers to determine the number of parallel pixel transfers, Y (see Figure 1 for reference). A source in the middle of the chip would have Y=1024 transfers. The maximum possible transfers is Y=2048. (Note for drizzled frames with pixel scale unity, the difference between input and output pixel transfers is negligible). Users also must determine the modified Julian date from the headers. We encourage users to verify that they are calculating the CTE corrections correctly using Figures 5 and 6 as examples, and being careful to match the formula parameters described in these figures' labels and captions.

7. Future Projections

It is always dangerous to try and predict the future, especially with such a brief view of the past. Still, for planning purposes we may use our global CTE correction formula and its time-dependence to extrapolate to the expected size of future losses and corrections. To do this we chose a few representative science applications and illustrate the estimated future losses to their sources in Figure 7. The parameters of the science applications we used are given in Table 3. We chose the position in the middle of each WFC chip (y=1024) to be the typical position of a source.

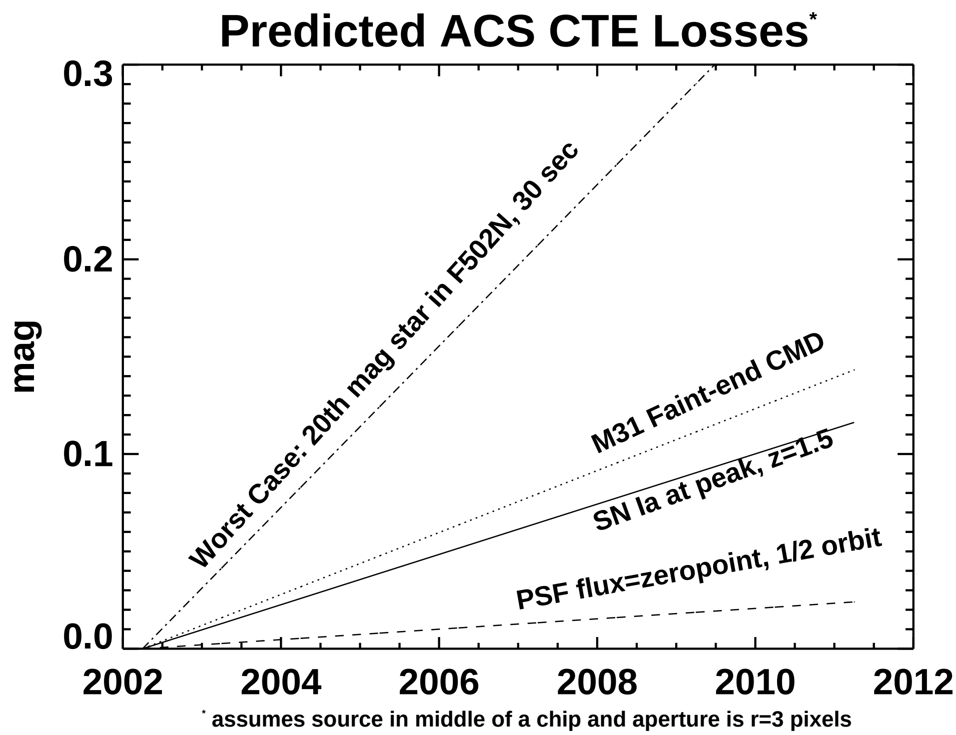

Figure 7: Projected CTE losses (and equivalently, the size of corrections) for example science applications described in Table 3. The precision of measurements is not limited by the size of the loss but rather its uncertainty. As a rule of thumb we suggest that the ultimate limit of precision will be ~25% of the loss after correction.

Table 3: Example Science Applications and their Assumed Parameters

Science Application	source flux (e)	sky (e)
SN Ia at peak z=1.5	100	30
M31 faint-end of CMD	40	100.
PSF, 1e/s, 1/2 orbit	1000	40
F502N, 30 sec, 20th mag star	258	0.1

Because background mitigates CTE, for most of the likely science applications which involve long integrations with efficient, broad filters, the expected impact of future CTE degradation is limited and manageable. For two specific examples, we chose high-redshift SNe Ia and resolved stellar populations in M31. By the end of the decade (e.g., 2010) the size of the typical loss and correction for these programs should be ~0.1 mag. It is important to remember that it is not the *size* of the correction which limits the precision of science applications, but rather its *uncertainty.* (A caveat to this statement is: if CTE losses are so severe, the camera *sensitivity* may be reduced, but this is not anticipated for most science applications). The uncertainty is likely to be a small, fixed fraction of the correction. As the set of calibration data grows, the uncertainty will decrease. Experience from WFPC2 indicates that it is unlikely to drop by more than ~25% of the correction itself due to differences in methods of measuring photometry (Whitmore, private communication). As a result, we would expect an ultimate limit to the precision of photometry for our example programs of ~0.02-0.03 mag by the end of the decade. Applications which seek to measure brighter stars, such as a star whose apparent magnitude matches the zeropoint of the filter (i.e., count rate=1 electron per second) in broad filters will be even less impacted, as seen in Figure 7. The reduction in photometric accuracy for these applications is negligible.

The worst case arises from short integrations in narrow band filters of relatively faint stars. As an example, we considered the F502N filter in a 30 second integration which yields an average of only 0.1 electrons per pixel in the sky. Even a star as bright as 20th mag in this filter will yield few counts in a short exposure and the net loss due to CTE may reach ~0.4 mag by the end of the decade. Using our previous rule of thumb, a measurement of such a source may be uncertain at the 0.1 mag level. We stress that the observing parameters of this worst case scenario will rarely, if ever, occur in a real science application (especially since the buffer dumps in ACS WFC discourage the use of such short exposures). In addition, observations closely matching our worst case scenario may be improved by utilizing the post-flash capability to add trap filling background counts (i.e., a “fat zero”). We are currently analyzing calibration data taken in this way and expect that post-flashing will reduce the systematic uncertainty of the photometry (at the price of increased statistical uncertainty due to shot noise).

We conclude that for real science applications, the use of CTE correction formulae should limit the precision of flux measurements of typical faint sources to no worse than a few percent by the end of the decade. This level of uncertainty should be quite manageable for the vast majority of science programs. Programs seeking to measure single sources (i.e., not observing in survey mode but rather following choice targets) can further mitigate the impact of CTE by placing targets near the read-out amplifier.

Acknowledgements

We wish to thank Stefano Casertano, Brad Whitmore, John Krist, Ron Gilliland, and Roeland van der Marel for helpful consultations, and the ACS+WFPC2 Branch for commenting on earlier versions of these results.

References

Riess, A. 2003, ISR ACS 03-009
Whitmore, W., Heyer, I. and Casertano, S. 1999, PASP, 111, 1559
Goudfrooij, P. and Kimble, R. A. 2002, HST Calibration Workshop, page 105